JOURNAL OF MATERIALS SCIENCE 31 (1996) 4233–4240

Synthesis of yttrium iron garnet precursor particles by homogeneous precipitation

Y. S. AHN, M. H. HAN
Energy Material Laboratory, Korea Institute of Energy Research, Taedok Science Town, P.O. Box 5, Taejon 305-343, Korea

C. O. KIM
Department of Material Engineering, Chung Nam National University, Taejon, Korea

Yttrium iron garnet (YIG) precursor particles were obtained by homogeneous precipitation in a nitrate salt solution by a reaction involving the thermal decomposition of urea. Chemical analysis indicated that solid phases were initially precipitated with sequential iron ion content. The precipitate formed was an amorphous mixed iron oxide phase. The complex composition and the thermal decomposition of the precipitate were studied by thermogravimetry–differential thermal analysis, differential scanning calorimetry, X-ray diffraction, and Fourier transform–infrared spectroscopy. Precipitate morphology was observed by SEM and TEM. Fine-grained single-phase yttrium iron garnet (YIG: $Y_3Fe_5O_{12}$) powders were obtained by calcination of the precipitate at 1200 °C. $YFeO_3$ intermediate compound was formed at 600 °C prior to the final crystallization of YIG.

1. Introduction

Yttrium iron garnet (YIG: $Y_3Fe_5O_{12}$) is the most representative and well-known compound among the rare-earth iron garnets. YIG is a ferrimagnetic material which is used as filter in microwave circuitry, electronic resonators and lasers [1].

The conventional solid mixture for the preparation of YIG powders involves a high temperature, resulting in the loss of the fine particulate nature. A variety of processing techniques has been investigated to form single-phase YIG powders, including coprecipitation, hydrolysis of metal alkoxides, amorphous citrate gel, spray-drying, freeze-drying, evaporation/decomposition and aerosol synthesis. In general, coprecipitation [2–5], the sol–gel method using an amorphous citrate gel [6–8], and the hydrolysis of metal alkoxides [9–13] have been widely used to prepare YIG powders. The sol–gel method yields very fine, active and contamination-free powders. However, the alkoxide hydrolysis process is tedious, with low yield and high cost. In a typical chemical procedure, their particles were obtained by adding a basic solution, such as ammonia, directly to the solution containing metal cations. This coprecipitation method is very difficult to control during the processing because of the rapid change of the solution concentration and the localized and discontinuous nature of the introduction and reaction of the anion species [14].

A better control can be obtained if the anion species, and hence precipitate, are generated simultaneously and uniformly throughout the solution. This process is called a homogeneous precipitation method. The basis of this method is the slow introduction of anion species into the solution until the solubility limit is exceeded. Urea, which can slowly decompose to yield ammonia and carbon dioxide, may be used as the anion source of ammonia [14, 15].

Recently, Haneda *et al.* [16] described ytterbium iron garnet powders synthesized by homogeneous precipitation using urea. Fuita and Kayama [17] and Akinc *et al.* [18], reported the synthesis of Mg^{2+}/Al^{3+}, Y^{3+}/Al^{3+} mixed compound powders using this method.

In the present work, we studied the precipitation of yttrium and iron cations from an aqueous solution by the thermal decomposition of urea and the conversion of the precipitate to yttrium iron garnet upon calcination at various temperatures.

2. Experimental procedure

2.1. Materials and solution preparation

The starting materials were $Y(NO_3)_3 \cdot 5H_2O$ (99.9%), $Fe(NO_3)_3 \cdot 6H_2O$ (99.9 %) and urea (99 %). Other reagents employed in the process, such as nitric acid and ammonium hydroxide, were reagent grade. The yttrium and iron stock solution were prepared by dissolving the corresponding nitrate salt in doubly distilled water at room temperature. The molarities of yttrium and iron stock solution were 0.4 and 2.5, respectively. In particular, the iron stock solution was prepared in a high concentration which was sufficiently acidic so that no hydrolysis could be detected at room temperature [19].

Initially, precipitation experiments were performed using individual cation solutions in order to

0022–2461

TABLE I Initial total cation and urea concentration, urea/cation ratio examined in this study and theoretical amounts of urea

Batch	$[Y^{3+} + Fe^{3+}]$ (M)	[Urea] (M)	[Urea]: $[Y^{3+} + Fe^{3+}]$	[Theoretical amount of urea] (M)
1	0.032	1.0	31.3	0.048
2	0.096	1.0	10.4	0.144
3	0.160	1.67	10.4	0.240
4	0.224	2.33	10.4	0.336
5	0.320	3.33	10.4	0.480

observe powder morphology and precipitation characteristics of each system. The yttrium precipitation solution was obtained by adding 45 ml 0.4 M stock solution with 11.26 g urea to doubly distilled water to make a total volume of 500 ml clear solution. The concentrations of yttrium and urea in this solution were 0.036 M and 0.375 M, respectively. The iron precipitation experiment was performed using a solution consisting of 0.060 M iron and 0.625 M urea concentrations. These solutions were heated in a water bath to about 90 °C and held at that temperature. Ageing was continued after the first visible signs of precipitation.

Subsequently, precipitation experiments were carried out using the mixed solution of yttrium and iron by changing the total cation and urea concentrations. However, a constant stoichiometric Y : Fe ratio of 3 : 5 was maintained. The pH of this solution was adjusted to 2.0 with nitric acid and ammonium hydroxide. The ranges of cation and urea concentrations studied are indicated together with the resulting urea/cation ratio and theoretical amounts of urea in Table I. The theoretical values were calculated using the following assumed reaction [17]

$$3Y(NO_3)_3 + 5Fe(NO_3)_3 + 12(NH_2)_2CO \xrightarrow{+24H_2O}$$

$$Y_3Fe_5O_{12} + 12(NH_4)_2(NO_3)_2 + 12CO_2 \quad (1)$$

Similarly, the mixed solutions of yttrium and iron were heated and aged for different durations. The amount of urea added was 7–21 times of calculated theoretical value, to provide sufficient decomposition throughout the solution containing metal cations. The pH and temperature of the solution were monitored during the experiments. Visible signs of precipitation could be clearly observed as the bath was made of glass. After ageing was completed, the solution was quenched in cold water in order to prevent the decomposition of urea, and separated from the supernatant by centrifugation. The obtained precipitate was washed three times with distilled water and acetone and then dried overnight in a vacuum oven at 80 °C.

2.2. Characterization

The morphology of the precipitate was observed by scanning electron microscopy (SEM, Philips XL-30, Netherlands). Transmission electron microscopic (TEM; Philips CM12, Netherlands) observation was carried out on the precipitate deposited on a carbon substrate. Analysis of precipitate composition was performed by a combination of inductively coupled plasma atomic emission spectroscopy (JY38 Plus, France) for total yttrium and iron, inert gas fusion for total oxygen (Leco TC-436, America), and combustion chromatography (Leco TS-444, America) for total carbon. Infrared spectra (FTIR; Nicolet ODXB, America) on the precipitate were recorded from 400–4600 cm^{-1} using the KBr pellet method. Thermal analysis of the precipitate was conducted using simultaneous thermogravimetry and differential thermal analysis (TG–DTA; Netzsch STA409, Germany), and differential scanning calorimetry (DSC; Netzsch STA409, Germany) in air at a heating rate of 4 °C min^{-1}. X-ray diffraction patterns (XRD; Rigaku RTP300RC, Japan) of the precipitate and the heat-treated powders were investigated using iron-filtered CuK_α radiation in the range 20 °–90 °.

3. Results and discussion

3.1. Precipitation characterization

The concurrent temperature and pH level of the precipitation process are indicated in the respective figures. Yttrium and iron individual cation precipitation experiments are shown in Fig. 1, and the precipitation experiments of the mixed solution of yttrium and iron are shown in Fig. 2. The data were obtained under conditions where sufficient urea was added to maintain a constant [urea]/[cation] ratio of 10.4. The experimental conditions of the individual cations were also the same as those for the yttrium and iron mixture. The starting pH of the solution was adjusted to bring all the solution to an initial pH value of 2.0. The decomposition process of urea can be represented by the following reactions [18]

$$(NH_2)_2CO + 4H_2O \rightarrow 2NH_4OH + H_2CO_3 \quad (2)$$

Then, the subsequent dissociation of the reaction products yields OH^- and CO_3^{2-} ions as the anion source. Hydroxyl carbonates may or may not form, depending upon the presence of other supporting anions and the solubilities of metal ions in the solution. Hydroxyl carbonates of the yttrium and aluminium mixture been prepared by this method using urea

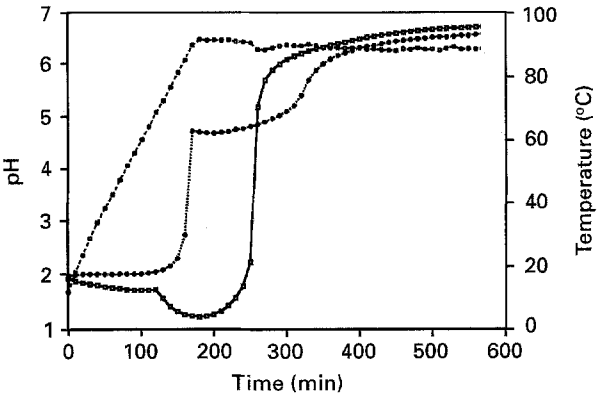

Figure 1 Variation of (□, ●) pH and (○) temperature with time for the individual (Y^{3+}, Fe^{3+}) precipitation processes. (—■—) pH [0.06 M Fe]; (···●···) pH [0.036 M Y].

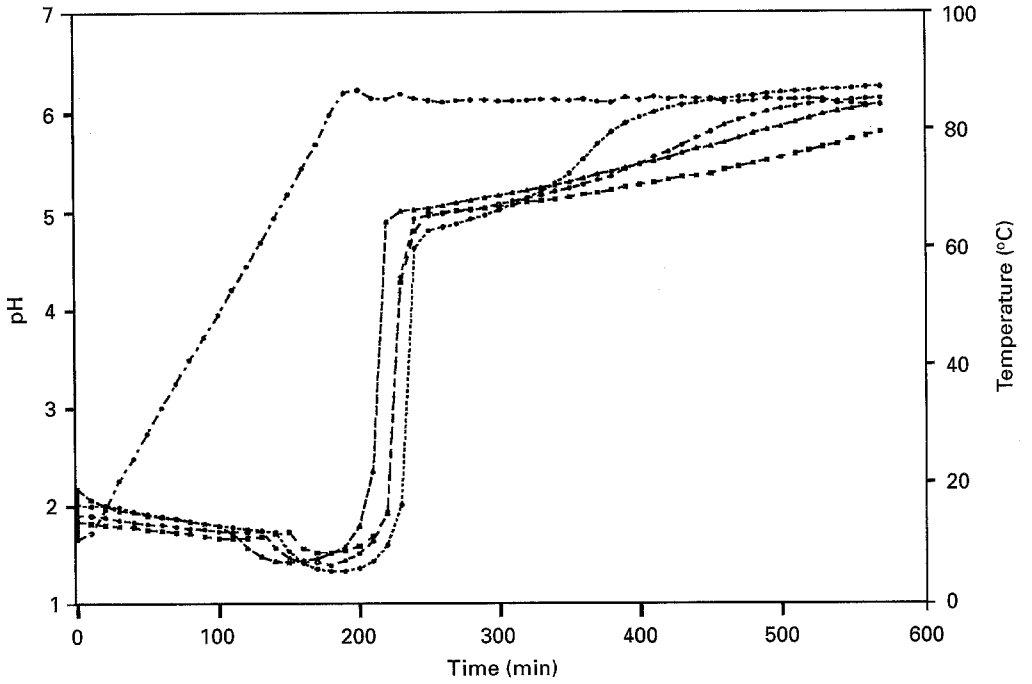

Figure 2 Variation of pH and (- — -●- — -) temperature with time for several mixed (Y^{3+}, Fe^{3+}) precipitation processes. pH: (---●---) [0.096 M], (---■--) [0.160 M], (---▲---) [0.224 M], (---■---) [0.320 M].

[18]. However, the ytterbium and iron mixture precipitate prepared using similar techniques by Haneda *et al.* [16], was described as merely the hydroxide form.

In the case of iron precipitation in Fig. 1, the initial slow decrease in pH together with heating of the solution were due to the formation of an intermediate produced from the decomposition of urea and an increase in the dissociation constant of water [15]. Then, the subsequent decrease in pH continued around pH 1.2. In this process, redish tints in the solution were observed from only one burst of nuclei [20, 21]. The occurrence of an iron precipitate, e.g. slight turbidity in the solution, began around pH 1.5. After the precipitation was completed, the pH stabilized as time passed, and then a sharp rise in pH was again observed. This rise in pH was attributed to the formation of ammonia and carbon dioxide by the decomposition reaction. Again the slow rise in pH can be caused either by slow decomposition of urea, releasing hydroxide ions, or deprotonation of hydrated metal ions.

Upon continued heating, the pH of the solution levelled off around 6.7 and remained almost constant during the ageing period. Also in the case of yttrium precipitation, the lower initial pH was due to acidic yttrium ions in the solution [15]. The pH increased little until about 80 °C, and then a sharp increase was observed. The sharp rise in pH was due to the rapid decomposition of urea as the temperature increased. At this time, a slight turbidity was observed as yttrium precipitation began to occur from about pH 4.7; then whitish tints in the solution were observed. The pH increased slowly around pH 5.1 and then rapidly up to pH 6.0. The pH remained relatively steady between 6.0 and 6.6. Additional ageing produced continuous growth of the precipitate. Yttrium precipitate could be obtained in the pH range between 4.7 and 6.6 due to sufficient dissociation of ammonia and carbonic acid to raise the pH. In the case of precipitation experiments using the mixed solution of yttrium and iron, each solution exhibited a similar pH rise and precipitation characteristic, despite the difference in total cation concentration. This was due to the constant [urea]/[cation] ratio, because the decomposition rate of urea is directly related to urea concentration. Even though the ratio of urea to cation was the same for all the solutions, the final pH of each solution decreased as the total cation concentration increased. The difference in the precipitation region shown in Fig. 2 was due to the concentration of total cations. Also, a slight deviation of the precipitation curve may be caused by the difference in heating rates, because the heating rate affects the decomposition rate of urea. The temperature curve shown in Fig. 2 was the average temperature of four solutions during the precipitation process. Precipitation characteristics of the yttrium and iron mixture were similar to those of the individual cations, as described above.

3.2. Supernatant characterization

In order to investigate the variation of individual cation concentrations with pH of the solution during the precipitation process, samples of the 0.096 M mixture solution were extracted from a 500 cm^3 batch at several times after the first visible sign of precipitation. The sample solutions, which were no longer clear, owing to solid-phase formation, were centrifuged to separate the precipitate. The resulting clear supernatants were analysed by ICP–AES for Fe^{3+} and Y^{3+} ion concentrations. The results are presented in Fig. 3. The initial concentrations of Fe^{3+} and Y^{3+} are marked at time zero. It was clear that iron ions began

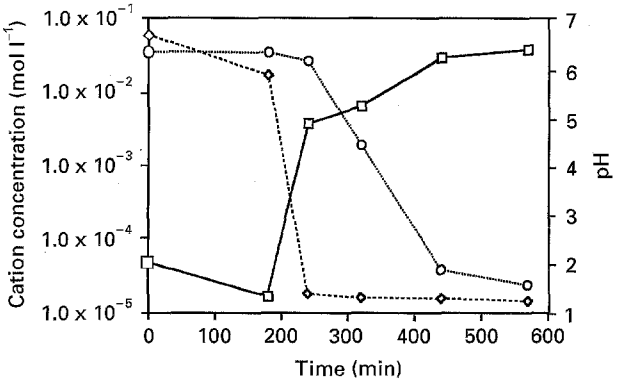

Figure 3 The variation of cation concentration with pH for a precipitation solution of 0.096 M. (···○···) [Y], (---◇---) [Fe], (—□—) pH.

to precipitate before the yttrium ions. At the time when a visible solid phase appears, iron ions had partially precipitated below pH 2, and the yttrium ions remained in the state of the initial concentration. At about pH 5, precipitation of iron ions had completed and a small amount of yttrium ions had precipitated. In the pH range 5.0–6.0, nearly all the yttrium ions had precipitated and precipitation was completed around pH 6.6. After the precipitation experiment was completed, analysis for residual Fe^{3+} and Y^{3+} ions in the clear supernatant revealed the ion concentration to be less than 30 p.p.m.

Alternative spectroscopic examination would possibly have provided more accurate information on the precipitation process. The data shown in Fig. 3 support the concept of sequential precipitation in this process.

3.3. Morphology of the precipitated particles

The morphology of the precipitated particles obtained from the individual cations, yttrium and iron, is shown in Fig. 4. The particles formed during the precipitation were gelatinous. The morphology of iron particles shown in Fig. 4a was very small and non-uniform. There appeared to be considerable agglomeration among the very fine particles. The morphology of the precipitate obtained from yttrium solution is shown in Fig. 4b. The precipitated particles were relatively uniform in size and spherical in shape. The average particle size was about 0.4 μm with a slight variation. There appeared to be some degree of agglomeration among the spherical particles, but these agglomerates were relatively weak and could easily be broken. The monosized, spherical morphology of yttrium precursor particles has been reported previously [15, 22].

It is interesting to compare the morphology of individual cation precipitates with that of the precipitate obtained from a mixed solution of yttrium and iron. The morphology of the precursor particles obtained from the mixed solution of yttrium and iron is shown in Fig. 5. The particles were very small and almost spherical in shape with agglomeration. The average particle size was larger than that of iron particles with

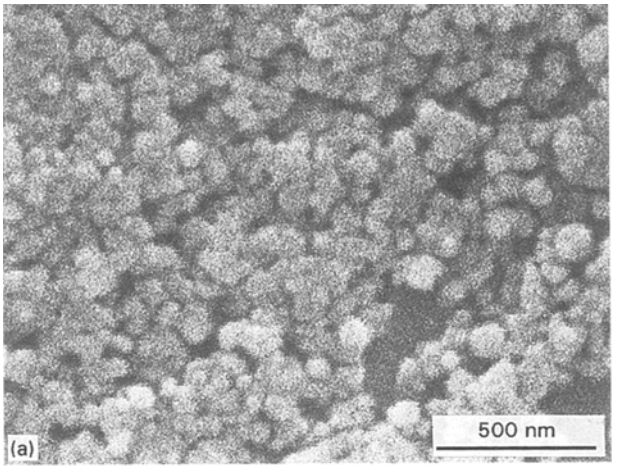

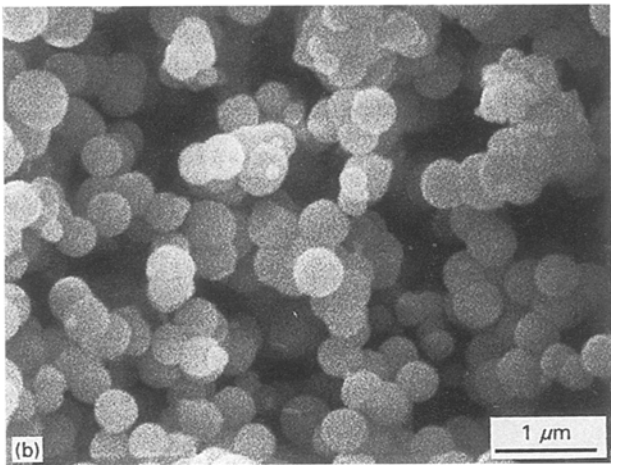

Figure 4 Scanning electron micrographs for particles of individual cations. (a) Iron: $[Fe^{3+}] = 0.06$ M, [urea] = 0.625 M; (b) yttrium: $[Y^{3+}] = 0.036$ M, [urea] = 0.375 M.

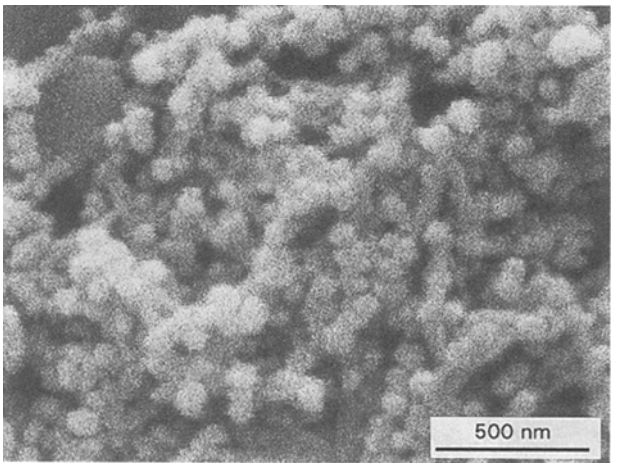

Figure 5 Scanning electron micrograph of mixed yttrium and iron particles of 0.096 M.

non-uniformity. The morphology of the particles shown in Fig. 5 was representative of the other particles obtained from the solution with the total cation concentrations listed in Table I. Similarly, those of other concentrations also produced gel-like precipitate. Note that the morphology of the mixture precipitate is similar to that of iron particles. The morphological similarity between the single iron particles

and the yttrium and iron mixture particles is possibly an indication that solid-phase formation did not occur by a coprecipitation process [18]; namely, the precipitation appeared to be sequential; iron ions precipitated first, followed by the yttrium ions. Haneda *et al.* [16] suggested the schematic representation of the formation process of the ytterbium iron garnet precipitate by observation of SEM and TEM, as shown in Fig. 6. Fig. 7 shows a transmission electron micrograph of the precipitated particles obtained from the total cation concentration, $[Y^{3+} + Fe^{3+}]$ of 0.096 M. It appeared that the mixed cation particles consisted of spherical primary particles, as described by Haneda *et al.*

The morphology of these particles after calcining at 1200 °C for 6 h is shown in Fig. 8. With increasing temperature, the particles formed clusters and agglomerates due to the localized growth, having a size of about 1 μm. It was seen that partially spherical particles existed separately between the clusters.

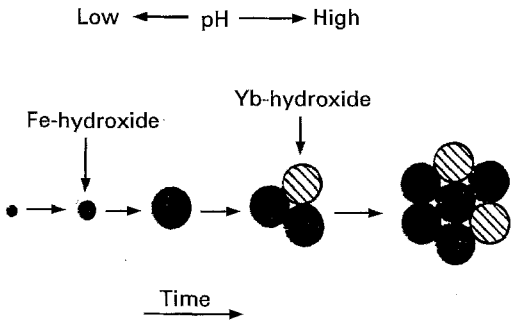

Figure 6 Schematic representation of the formation process of YbIG.

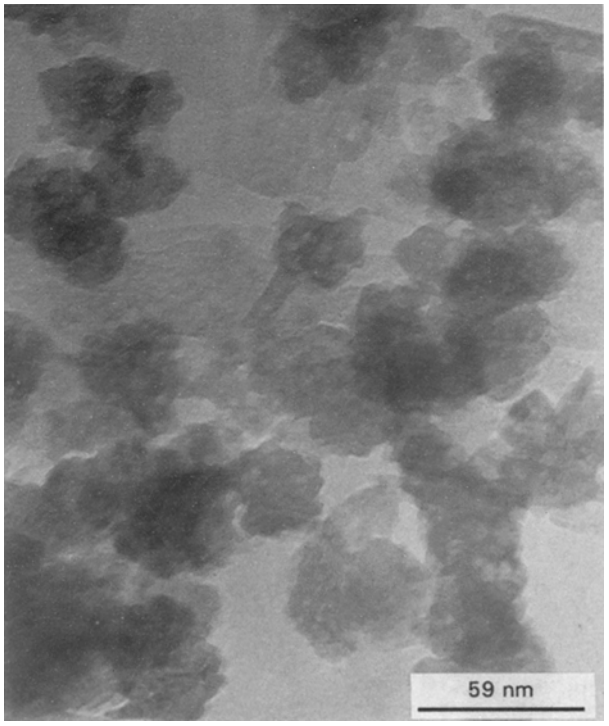

Figure 7 Transmission electron micrograph of mixed yttrium and iron particles of 0.096 M.

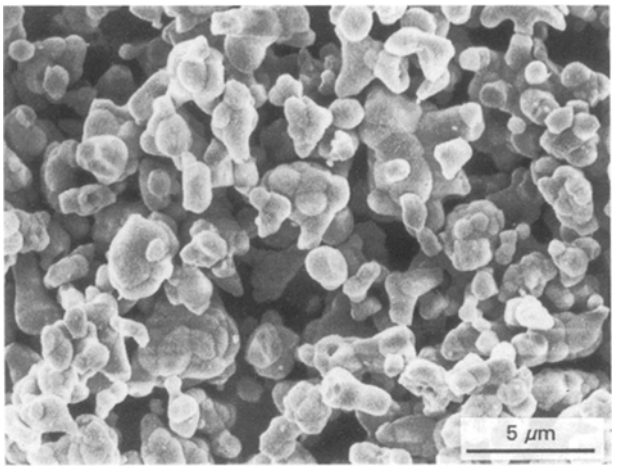

Figure 8 Scanning electron micrograph of mixed yttrium and iron particles of 0.096 M heat treated at 1200 °C.

3.4. Precipitate yield

The precipitated particles were calcined to 1200 °C for 6 h in air to form oxide compounds. The total recovered precipitate and oxide compounds formed after calcinating to 1200 °C were weighed to calculate the particle yield during the precipitation. The results of several experimental conditions are shown in Table II. It appeared that the yield increased with increasing $[\text{urea}]/[Y^{3+} + Fe^{3+}]$ ratio. The yield values from the solution with $[\text{urea}]/[Y^{3+} + Fe^{3+}] > 10.4$ were all around 93%, compared to the theoretical value. The critical value depended on securing complete recovery related to adequate urea content.

3.5. X-ray diffraction analysis

The precipitated particles obtained from the mixed solution of yttrium and iron were amorphous mixed iron oxide phase. Prior to investigation of phases existing in these particles, XRD analysis of individual yttrium and iron particles was carried out. The XRD patterns for individual yttrium and iron particles are shown in Fig. 9. The yttrium particles were amorphous phase (Fig. 9a), whereas the iron particles were found to be oxide phase (Fig. 9b). This intermediate phase is known as protohaematite, due to the presence of defects in the haematite lattice [23]. The recrystallization of protohaematite to the haematite phase occurred about at 280 °C, which was indicated by a well identified peak in the XRD pattern (Fig. 9c) and will be discussed in the TG–DTA studies. Kato and Morimitsu [24] reported that the haematite phase could be directly obtained from $Fe(NO_3)_3$ solution by homogeneous precipitation using urea. However, the existence of protohaematite was not described.

The crystallization behaviour of the 0.096 M YIG precipitated particles with subsequent heat treatment is shown in Fig. 10. Both particles dried at 100 °C and calcined at 300 °C indicated weak diffraction patterns corresponding to iron oxide phase, together with amorphous phase. The particles calcined up to 600 °C were found to form a small amount of $YFeO_3$ with the mixture of Fe_2O_3 and Y_2O_3. The diffraction pattern corresponding to $YFeO_3$ phase showed the most

TABLE II Precipitate yield obtained from the mixed cation solution

Batch	[Urea]/[Y^{3+} + Fe^{3+}]	Yield (%)
1	31.3	95
2	10.4	94
3	10.4	93
4	10.4	93
5	10.4	93

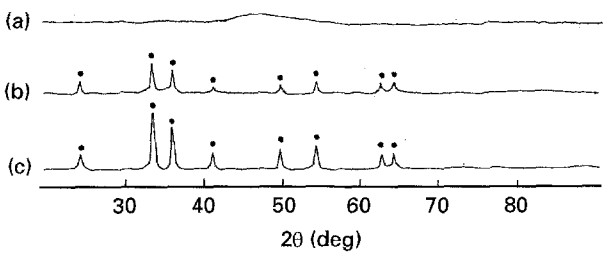

Figure 9 X-ray diffraction pattern of individual cation (Y^{3+}, Fe^{3+}) precipitates. (a) Yttrium precipitate dried at 80 °C: [Y^{3+}] = 0.036 M, [urea] = 0.375 M. (b) Iron precipitate dried at 80 °C: [Fe^{3+}] = 0.06 M, [urea] = 0.625 M. (c) Iron precipitate heat-treated at 300 °C.

intense reflection at 900 °C. The diffraction line of YIG phase began to appear when the calcination temperature was raised to 650 °C, and became sharp at 1000 °C, indicating that the crystallization of YIG proceeded very rapidly above 1000 °C. At the calcination temperature of 1000 °C, YIG and YFe_2O_3 with a small amount of Fe_2O_3 were present together. As the temperature was raised to 1100 °C, the intensity of YIG increased, the intensities of YFe_2O_3 and Fe_2O_3 decreased, and Fe_2O_3 only existed as traces. On increasing the temperature further, a diffraction line corresponding only to the YIG phase appeared after calcining at 1200 °C.

The relatively low temperature of crystallization and a single-phase crystallization may be attributed to the extremely fine scale of the primary particles. From the results of XRD studies, the garnet formation process can be described by the following reactions

$$Y_2O_3 + Fe_2O_3 \rightarrow 2YFeO_3$$

occurring at about 600 °C (3)

$$3YFeO_3 + Fe_2O_3 \rightarrow Y_3Fe_5O_{12}$$

completed at about 1200 °C (4)

The yttrium orthoferrite ($YFeO_3$) crystallization began near 600 °C, and was completed around 900 °C; the YIG crystallization began near 650 °C, and was completed at about 1200 °C. This result also suggested that the YIG crystallization occurred by a solid-state reaction of $YFeO_3$ and Fe_2O_3 in the temperature range 650–1200 °C.

3.6. Chemical composition

Chemical analysis was combined with the FT–IR data to determine an approximate chemical formula for the precipitate with a total cation concentration of 0.096 M.

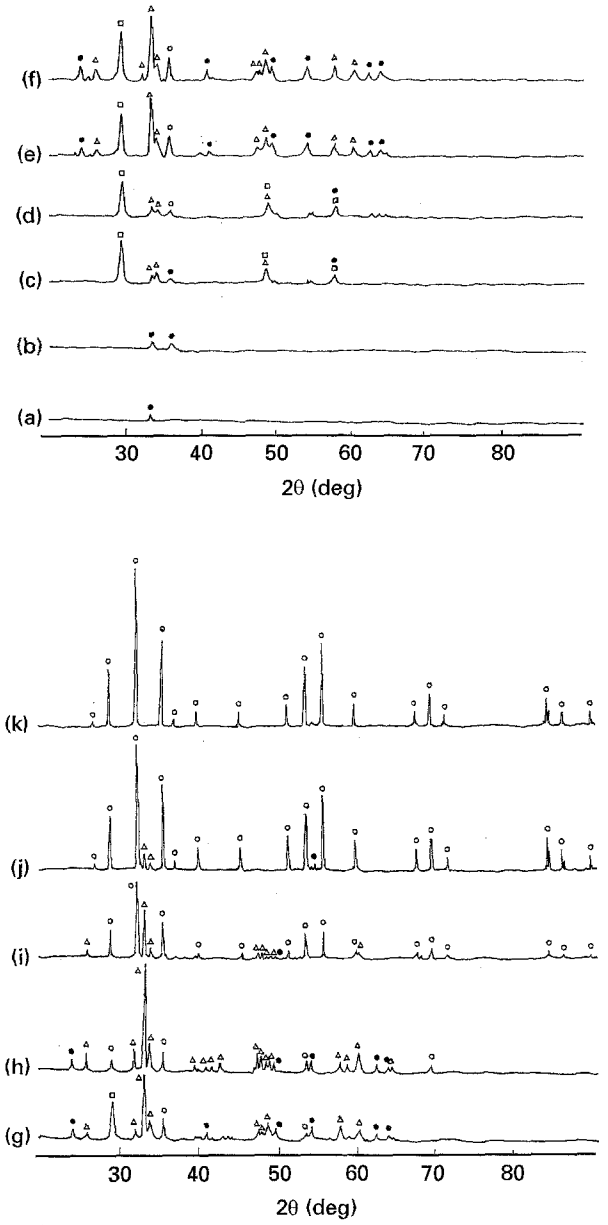

Figure 10 X-ray diffraction patterns for mixed cation (Y^{3+} + Fe^{3+}) precipitates of 0.096 M heat-treated at various temperatures for 6 h in air. (a) Dried precipitate, (b) 300 °C, (c) 600 °C, (d) 650 °C, (e) 700 °C, (f) 750 °C, (g) 800 °C, (h) 900 °C, (i) 1000 °C, (j) 1100 °C, (k) 1200 °C. (○) $Y_3Fe_5O_{12}$, (△) $YFeO_3$, (●) Fe_2O_3, (□) Y_2O_3.

The IR spectra of the precipitate are shown in Fig. 11. The IR band in the region 3660–2840 cm^{-1} may be due to the presence of water, because very broad, intense O–H stretching absorption occurred in this band region [7, 25]. The strong bands at 1390 and 1510 cm^{-1} corresponded to the carbonate band. The splitting antisymmetrical band indicated that the carbonate had C_{2v} symmetry and was acting as a bidentate ligand [26]. The weak band at 840 cm^{-1}, which was associated with the out-of-plane bending of CO_3^{2-}, further confirmed the presence of the carbonate [27]. The broad bands at 470 and 560 cm^{-1} were known as protohaematite [28, 29]. Table III presents the results of the chemical analysis of the precipitate and total weight loss, together with the calculated values based on the following assumptions. It was initially assumed that the precipitate could be some forms of hydroxyl carbonate of yttrium with some

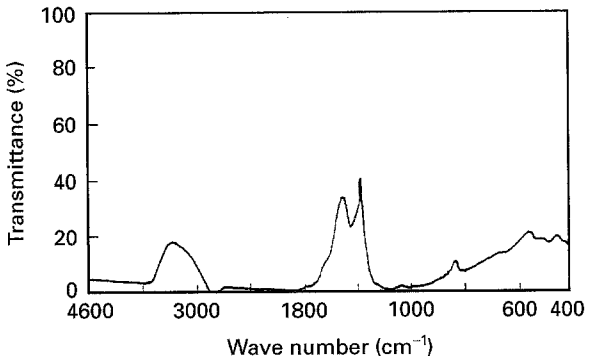

Figure 11 Infrared spectra for a mixed cation (Y^{3+} + Fe^{3+}) precipitate of 0.096 M.

TABLE III Chemical analysis of precipitate and calculated values

Elements	Experimental results				Calculated result
	(wt %)	Ionic species	(wt %)	(mol)	(wt %)
Y	25.1	Y^{3+}	25.1	0.28	25.6
Fe	27.0	Fe^{3+}	27.0	0.48	26.8
O	40.2	$(OH^-)^a$	11.6	0.68	41.6
C	4.5	CO_3^{2-}	22.5	0.38	4.7
LOI	26.4				24.4

[a] Calculated from total oxygen $-(CO_2)$ $-$(oxygen of Fe_2O_3).

degree of hydration. The iron ion precipitate was oxide in form. This assumption was based on the previous study with yttrium ion [15], and mixed yttrium and aluminium [18] precipitated by urea which formed a hydroxyl carbonate. The chemical formula was assumed to be $2.5Fe_2O_3 \cdot Y_3(OH)_{9-2x}(CO_3)_x \cdot nH_2O$. The ratio of iron to yttrium was stoichiometrically constant and x was calculated using total carbon. The coefficient of water was calculated from the excess hydroxide over which charge neutrality was required. When the results of chemical analysis were combined with electrical neutrality requirements of the precipitate, the approximate chemical formula, $2.5Fe_2O_3 \cdot Y_3(OH)_{0.8}(CO_3)_{4.1} \cdot 6.5H_2O$ could be obtained. The results showed fairly good agreement between analytical and theoretical values. The loss on ignition value for the precipitate [18] was found to be around 26.4 wt % which was a little high compared to the calculated value of 24.4 wt %. The difference was probably due to incomplete accounting for oxygen in the analysis and the variation in the weight loss value as a function of drying history. The molarity ratio of iron to yttrium was quite close to the theoretical value of 0.6 for stoichiometric YIG. It was expected that the stoichiometric ratio would be preserved, because the batch-yield experiments showed that essentially all the metal cations came from solution during the precipitation.

3.7. Thermal analysis

TG–DTA and DSC analyses were performed on particles obtained from solution with the total cation concentration of 0.096 M. The simultaneously recorded TG–DTA and DSC data for the particles are shown, as representative examples, in Figs. 12 and 13. The precipitate formed was an amorphous mixed oxide phase, as mentioned before. Thermal decomposition of the particles in air consisted of several steps. The dehydration took place up to about 180 °C, showing two endothermic peaks. Thermograms showed a weight loss of 5 wt % corresponding to removal of absorbed and hydrated water [7, 25]. The first exotherm, at 260 and 280 °C, corresponded to the recrystallization of protohaematite to haematite [23] and was characterized by a well-defined exothermal effect. In the temperature range 180–500 °C, a weight loss of about 12 wt % occurred due to the reaction to form oxycarbonate of yttrium, included the evolution of CO_2 gas and water vapour [7, 25]. There were two endothermic peaks at 500 and 600 °C. The first endothermic peak at 500 °C was associated with the formation of oxycarbonate of yttrium [15]. The second peak, at 600 °C, represented the conversion of oxycarbonate to yttrium oxide [15]. A weight loss of 8 wt % between 500 and 600 °C occurred due to the decomposition of oxycarbonate related to the evolution of CO_2 gas. Weight loss up to 700 °C was very little, possibly indicating that only residual oxycarbonates of yttrium are decomposing [12]. An exothermic peak at 740 °C showed the crystallization

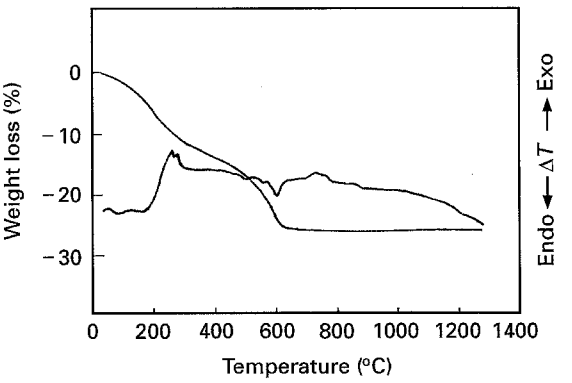

Figure 12 TG-DTA curve for a mixed cation (Y^{3+} + Fe^{3+}) precipitate of 0.096 M.

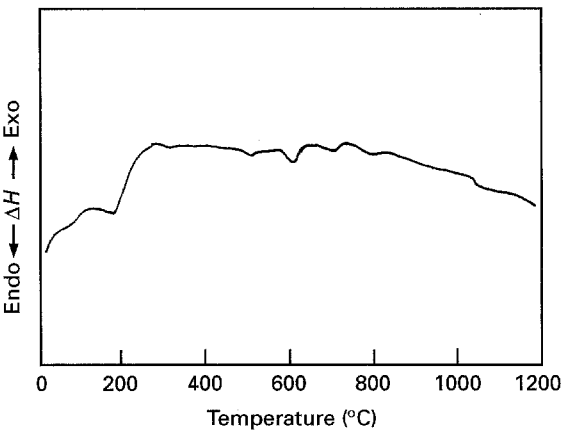

Figure 13 DSC curve for a mixed cation (Y^{3+} + Fe^{3+}) precipitate of 0.096 M.

of $YFeO_3$ and a small amount of YIG. It appeared that the crystallization temperature differed from that of the XRD results. This is due to the difference in the duration at measuring temperature, that is, the precipitate for XRD studies was maintained at the calcination temperature for 6 h, whereas the precipitate for thermal analysis had no duration at the corresponding temperature. The overall thermal decomposition of the precipitate can be approximately summarized by the following reaction

$$\text{Precipitate} \xrightarrow{180^\circ C} \underbrace{2.5Fe_2O}_{\text{(protohaematite)}} \cdot Y_3(OH)_{9-2x}(CO_3)_x \quad (5)$$

$$\xrightarrow{280^\circ C} \underbrace{2.5\,Fe_2O_3}_{\text{(haematite)}} \cdot Y_3(OH)_{9-2x}(CO_3)_x$$

$$\xrightarrow{500^\circ C} 2.5\,Fe_2O_3 \cdot Y_3O_y(CO_3)_x$$

$$\xrightarrow{600^\circ C} 2.5\,Fe_2O_3 + 1.5Y_2O_3$$

$$\xrightarrow{740^\circ C} YFeO_3 + \text{YIG (small amount)}$$

4. Conclusion

Yttrium iron garnet precursor particles were synthesized by homogeneous precipitation via the thermal decomposition of urea in hot nitrate salt solution. The precursor particles formed were an amorphous mixed iron oxide phase. The intermediate phase, known as protohaematite, followed conversion of haematite at about 280 °C. The existence of intermediate phase was ascertained by the exothermic peak at 280 °C corresponding to the recrystallization of protohaematite to haematite, and the well-defined XRD line shown for single iron particles calcined at 300 °C. The YIG particles obtained were very small and near to spherical in shape with agglomerates. The particles yielded highly reactive materials that formed the desired single-phase YIG compounds at relatively low temperature. The crystallization temperature for the formation of single-phase YIG was 1200 °C. It was also found that the YIG crystallization proceeded by a solid-state reaction of $YFeO_3$ and Fe_2O_3. The approximate chemical formula of the precipitate was $2.5\,Fe_2O_3 \cdot Y_3(OH)_{0.8}(CO_3)_{4.1} \cdot 6.5H_2O$. The thermal decomposition of the precipitate consisted of four major steps: dehydration, recrystallization of the protohaematite to haematite, decomposition of the yttrium hydroxyl carbonate to oxycarbonate, conversion of yttrium oxycarbonate to oxide.

Acknowledgement

The authors thank Professor Kwang Soo No, Korea Advanced Institute of Science and Technology, for reviewing this manuscript and for making valuable comments.

References

1. J. HELSZA, Jr. (ed.), "Yttrium Iron Garnet Resonators and Filters", (Wiley, New York, 1985).
2. V. P. CHALYI and K. P. DANIL'CHENKO, *Izv. Akad. Nauk SSSR Neorg. Mater.* **9** (1973) 1208.
3. K. RAVINDRAN NAIR, *Am. Ceram. Soc. Bull.* **60** (1981) 626.
4. N. I. MEZIN, E. N. KUZNETSOV and N. YU. STRAROSTYUK, *Izv. Akad. Nauk SSSR Neorg. Mater.* **25** (1989) 1187.
5. E. N. LUKACHINA, V. I. STETSENKO and I. V. ERMOLENKO, *ibid.* **14** (1978) 102.
6. V. K. SANKARANARAYANAN, N. S. GAJBHIYE and D. BAHADUR, *J. Mater. Sci. Lett.* **6** (1987) 281.
7. V. K. SANKARANARAYANAN and N. S. GAJBHIYE, *J. Am. Ceram. Soc.* **73** (1990) 1301.
8. T. HATTORI, Y. IWADATE and M. FUKUDA, *Jpn J. Chem. Soc.* **6** (1991) 754.
9. M. I. YANOVSKAYA, T. V. ROGOVA, S. A. IVANOV and N. V. KOLGANOVA, *J. Mater. Sci. Lett.* **6** (1987) 274.
10. O. YAMAGUCHI, Y. MUKAIDA and A. HAYASHIDA, *ibid.* **9** (1990) 1314.
11. O. YAMAGUCHI, H. TAKEMURA and M. YAMASHITA, *J. Electrochem. Soc.* **138** (1991) 1492.
12. C. D. VEITCH, *J. Mater. Sci.* **26** (1991) 6527.
13. A. BACHIORRINI, *Silicates Ind.* **5–6** (1990) 121.
14. P. L. CHEN and I-WEI CHEN, "Reactive CeO_2 Powders by the Homogeneous Precipitation Method", Department of Materials Science and Engineering, University of Michigan.
15. D. SORDELET and M. AKINC, *J. Coll. Interface Sci.* **122** (1988) 47.
16. H. HANEDA, T. YANAGITANI, A. WATANABE and S. SHIRASAKI, *Jpn J. Ceram. Soc.* **98** (1990) 285.
17. K. FUJITA and I. KAYAMA, *ibid.* **86** (1978) 433.
18. M. AKINC, M. L. PANCHULA and M. H. HAN, *J. Eur. Ceram. Soc.* **14** (1994) 123.
19. E. MATIJEVIC' and P. SCHEINER, *J. Coll. Interface Sci.* **63** (1978) 509.
20. E. MATIJEVIC', *Acc. Chem. Res.* **14** (1981) 22.
21. J. BLENDELL, H. K. BOWEN and R. COBLE, *Am. Ceram. Soc. Bull.* **63** (1984) 797.
22. J. L. SHI and J. H. GAO, *J. Mater. Sci.* **30** (1995) 793.
23. S. YARIV and E. MENDELOVICI, *Appl. Spectrosc.* **33** (1979) 410.
24. A. KATO and Y. MORIMITSU, *Jpn J. Chem. Soc.* **6** (1984) 800.
25. V. K. SANKARANRAYANAN and N. S. GAJBHIYE, *Thermochim. Acta* **153** (1989) 337.
26. S. D. ROSS, "Inorganic Infrared and Raman Spectra", 1st Edn (McGraw-Hill, London, 1972) p. 150.
27. C. N. R. RAO, "Chemical Applications of Infrared Spectroscopy" (Academic Press, New York, 1963).
28. N. HAKEEN, P. BASILY, M. MOHARAM and N. SAGN, *J. Mater. Sci. Lett.* **5** (1986) 4.
29. E. MENDELOVICI, R. VILLALBA and A. SAGARZAZU, *Mater. Res. Bull.* **17** (1982) 241.

Received 20 September
and accepted 15 December 1995